Superprism effect in opal-based photonic crystals

T. Ochiai and J. Sánchez-Dehesa
Departamento de Física Teórica de la Materia Condensada, Facultad de Ciencias (C-5), Universidad Autónoma de Madrid, Madrid 28049, Spain

(Received 11 July 2001; revised manuscript received 6 September 2001; published 10 December 2001)

This paper investigates the superprism effect in opal-based three-dimensional photonic crystals which consist of an face-centered cubic (fcc) array of close-packed dielectric spheres embedded in a host. The light propagation angle inside the opals is determined by the group velocity vector of the bulk eigenmodes having the strongest coupling with the incident light at the boundary of the opal. It is found that the superprism effect takes place quite generally in the frequency range where many flat bands exist owing to the zone folding. The numerical simulations of the superprism effect in bare opal systems indicate that the effect can be used as frequency selector devices as well as beam splitters.

DOI: 10.1103/PhysRevB.64.245113 PACS number(s): 42.70.Qs, 42.79.Bh, 42.25.Gy, 41.20.Jb

I. INTRODUCTION

Recently, photonic crystals (PC's) attract much attention due to their possible applications in light control devices. So far, studies of PC's have been focused on the photonic band gap in which the photon density of states is zero. In this region the propagation of the radiation field is forbidden and thus a variety of novel phenomena, e.g., inhibition of spontaneous emission,[1] are possible. A PC with a full photonic band gap resembles an insulator in which the Fermi energy lies in the energy gap. However, PC's have other application than just being used as photonic insulator, that is, they can be employed as novel photonic conductors. Light propagation inside PC's is quite different from that in ordinary materials. This is mainly caused by the anisotropy of the photonic dispersion relation which reflects the space group symmetry of the PC. The anisotropy is quite large even if the periodic modulation of the PC is weak. As Kosaka *et al.* showed,[2] the anisotropy can be utilized as the mechanism of the superprism effect, i.e., an extraordinary angle- and wavelength-sensitive light propagation. We know that ordinary prism are based on the wavelength dependence of the refractive index. Generally the dependence is small and the light propagation angle is determined by Snell's law. As a result, the angle- and wavelength-sensitivity is very limited. In a PC the sensitivity can be greatly enhanced by changing various of its parameters. In addition, the sensitivity can be also strongly modified by the geometry of the boundary surface.

So far, the superprism effect has been studied in two-dimensional (2D) PC's (Ref. 3) and auto-cloned three-dimensional (3D) PC's,[2,4] where the out-of-plane propagation was neglected. Recent progress in fabrication techniques has produced 3D PC's with various geometrical structures including simple cubic,[5] body-centered cubic,[6] and fcc (Ref. 7) structures. In these photonic crystals the 3D anisotropy in the photonic bands dispersion relation is very large and the out-of-plane propagation can not be neglected. Therefore, a careful analysis of the superprism effect in these PC's is in order.

In this paper the superprism effect is investigated in opal-based 3D PC's. These PC's consist of an fcc structure of closed-packed dielectric spheres embedded in a host with a different dielectric material. These photonic systems have several advantages in technological applications, being the more important the easy process of fabrication.[7] We are mainly interested in the correlation among the input and output light propagation angles as well as their frequency dependence. For simplicity, we will restrict our study to the response of light at two selected boundaries of the semi-infinite photonic crystal. At a given frequency of the incident light, since several bulk eigenmodes with different directions of propagation could be excited, we must know the modes with the strongest coupling with the incident light. In this work, we introduce an useful method to explore the coupling and then extract the most plausible direction of the light propagation in the PC by using the method. Whereas the correlation is very complicated, several common features of the light propagation are obtained.

The paper is organized as follows. In Sec. II the kinetic matching condition between the incident light and bulk eigenmodes in the PC is derived by using the concept of the surface Brillouin zone (SBZ). Branching ratio of the bulk eigenmodes at a given incident light is explored in Sec. III. Results of numerical simulations of the superprism effect are discussed in Sec. IV. Finally, in Sec. V we summarize our results.

II. KINETIC MATCHING CONDITIONS

The opal-based PC's can be classified in three main categories according to the dielectric materials in the spheres and in the host. (1) Bare opals, in which silica spheres with dielectric constant 2.1 are embedded in air, are the simplest opal-based PC's.[7] These systems have no omnidirectional photonic band gap. Besides, since the index contrast between the spheres and air is very small, the photonic band structure is quite similar to that of the empty lattice model with infinitely small periodic modulation. (2) Loaded opals, in which the air voids of the bare opals are in-filled with another dielectric material such as a polymer[8] or with a semiconductor such as Si,[9] Ge,[10] CdS,[11] etc. The photonic properties could be enhanced with respect to the bare opal systems if the dielectric contrast between silica and the in-filled materials is increased. (3) Inverse opals, which are obtained when the silica in the loaded systems is dissolved by chemical means. In these systems one can reach the maximum dielectric con-

trast and an omnidirectional band gap could be obtain if the material infiltrated has a dielectric constant high enough.[12,13] As was mentioned before, the opal-based PC's have the close-packed fcc structure of dielectric spheres and thus the filling fraction of spheres is about 0.74.

In principle, one might consider that bare opals have a weak anisotropy in the dispersion relation because of its small index contrast. However, it is not the case because the anisotropy is caused by the symmetry of the space group which exists even if the periodic modulation is weak.

Let us consider the symmetries of the dispersion relation in the opal-based PC's. The eigenfrequency $\omega(\mathbf{k})$ with Bloch wave number vector $\mathbf{k}$ within the first Brillouin zone (BZ) has the following symmetries:

$$\omega(R\mathbf{k}) = \omega(\mathbf{k}), \tag{1}$$

$$\omega(\mathbf{k}+\mathbf{G}) = \omega(\mathbf{k}), \tag{2}$$

where R is an element of the O_h group, which is the point group of the fcc structure of spheres, and $\mathbf{G}$ is the reciprocal lattice vector of the fcc structure. Since the group velocity $\mathbf{v}(\mathbf{k})$ is the gradient of $\omega(\mathbf{k})$, similar equations hold for the group velocity

$$\mathbf{v}(R\mathbf{k}) = R\mathbf{v}(\mathbf{k}), \tag{3}$$

$$\mathbf{v}(\mathbf{k}+\mathbf{G}) = \mathbf{v}(\mathbf{k}). \tag{4}$$

These equations give a severe restriction to the light propagation irrespective of details of the system. For example, if $\mathbf{k}$ is on a mirror plane in the BZ, the normal component of the group velocity to the plane is zero. Thus, the group velocity vector must be parallel to the plane. On a high symmetric axis in the Brillouin zone, e.g., Λ (i.e., the Γ-L interval), several mirror planes intersect each other. This means that the group velocity vector must be parallel to the intersection lines and thus parallel to the axis concerned. Since the group velocity vector of an eigenmode gives the direction of propagation of the eigenmode, the direction of the light propagation is also parallel to the axis.

In order to get the response of light inside these PC's, effects at the air/opal interface must be incorporated, because the superprism effect stems from the boundary of the PC. For simplicity, we assume a semi-infinite opal-based PC whose boundary is normal to a certain direction. Strictly speaking, in this case the spatial symmetry of the photonic crystal reduces to a 2D one. However, the arguments given above are still employed as far as properties of the eigenmodes in bulk are concerned. In what follows we focus on the photonic crystals with the boundary normal to the (111) or (001) direction. In the (111) case the photonic crystal can be regarded as a semi-infinite stack of monolayers that are composed of the triangular array of dielectric spheres with period $a/\sqrt{2}$. Here, a is the period of a cubic cell of the fcc lattice. There is the C_{3v} symmetry in the plane normal to (111). In the (001) case the stack of monolayers of spheres, whose periodicity is the square lattice with period $a/\sqrt{2}$, forms the photonic crystals. In this case, C_{4v} is the relevant symmetry group.

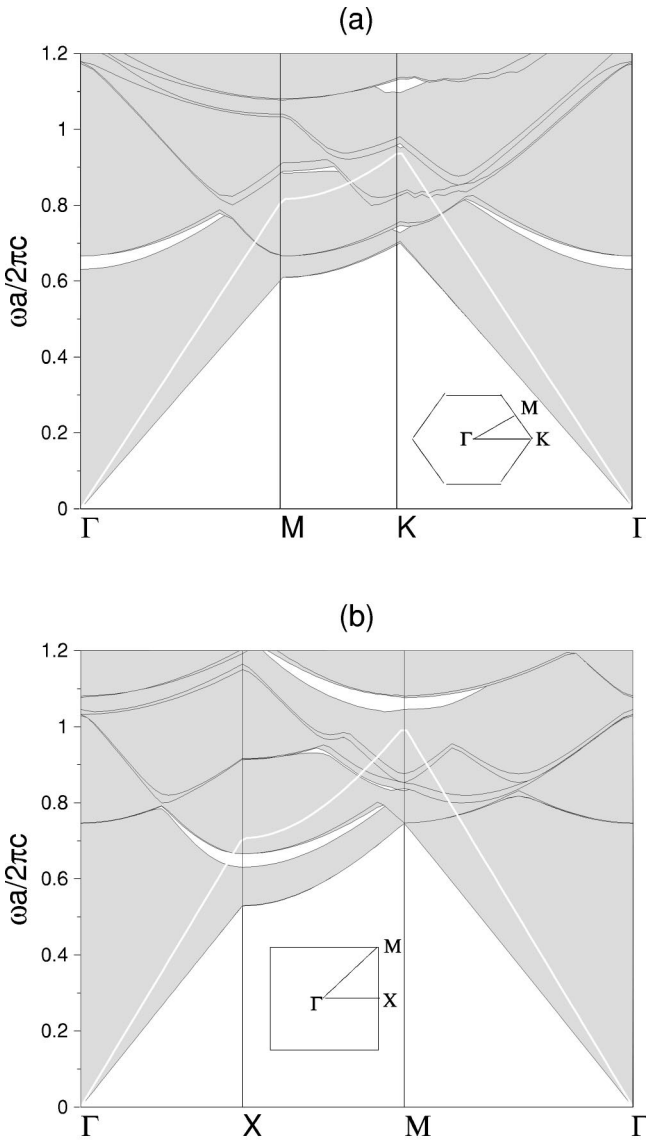

FIG. 1. (a) Projection of the photonic band structure of the bare opal on the SBZ of the fcc (111) surface. (b) Projection on the SBZ of the (001) surface. The corresponding SBZ's are shown in the insets. The shaded regions defines the bulk eigenmodes. The external radiation field exists above the light line which is represented by the thick white line.

As mentioned before, the photonic crystal still has a 2D translational symmetry. Thus, the reduced wave vector in the surface Brillouin zone (SBZ) as well as frequency is conserved. The SBZ, which is defined by the Wigner-Seitz cell of the 2D reciprocal lattice associated with the boundary surface, is an efficient notion to analyze PC with a boundary.

In order to see how the eigenmodes couple to the incident light, it is important to project the bulk photonic band structure on the SBZ. Typical projected band diagrams are shown in Figs. 1(a) and 1(b), which represent the projection of the photonic band structure of the bare opal on the SBZ associated to the fcc (111) and (001) boundary surfaces, respectively.

In Fig. 1 the shaded regions correspond to the allowed

frequency region of the bulk eigenstates and the thick white line defines the light line, above which the external plane wave is allowed to exist. The blank regions above the light line represent pseudogaps. The incident light in a pseudogap cannot enter into the photonic crystal. For example, the incident light with the reduced wave vector lying near the K point of SBZ of the fcc (111) surface cannot couple with bulk eigenmodes if its frequency is around $\omega a/(2\pi c)=1.1$.

The group velocity of the bulk eigenmodes gives another criterion on the coupling. Physically, the eigenmode with negative v_z (we take the z direction to be normal to the boundary and the photonic crystal is in $z>0$) should be neglected. Thus, only the bulk eigenmodes with positive v_z can couple with the incident light.

To summarize, the kinetic matching conditions between the bulk eigenmodes and the incident light are given as follows. (a) The frequency and the reduced wave vector in SBZ are conserved. (b) The bulk eigenmodes are above the light line. (c) v_z is positive. If these conditions are satisfied, the incident angles $(\theta_{\rm inc},\phi_{\rm inc})$ and the propagation angles in the photonic crystal $(\theta_{\rm out},\phi_{\rm out})$ are given by

$$\mathbf{k}=\frac{\omega}{c}(\sin\theta_{\rm inc}\cos\phi_{\rm inc},\sin\theta_{\rm inc}\sin\phi_{\rm inc},\cos\theta_{\rm inc}), \tag{5}$$

$$\mathbf{v}=|\mathbf{v}|(\sin\theta_{\rm out}\cos\phi_{\rm out},\sin\theta_{\rm out}\sin\phi_{\rm out},\cos\theta_{\rm out}), \tag{6}$$

where $\mathbf{k}$ is the wave vector of the incident light.

III. BRANCHING RATIO

In the previous section we focused on the kinematics across the air/opal interface and did not take account any matching condition for the fields at the boundary. At low frequencies a couple of bands are almost degenerate because they originate from two independent polarizations at a given wave number vector in free space. Thus, for the incident light with a certain polarization the overcounting of the bulk eigenstates happens if only the kinetic matching conditions are taken into account. Moreover, at high frequencies several bulk eigenmodes are kineticly matched to the incident light (see Fig. 3). The coupling strength between these eigenmodes and the incident light differs from mode to mode. We expect that only a few eigenmodes are strongly coupled with the incident light. Otherwise, the superprism effect is quite difficult to handle. This is not an optimistic expectation, but numerical simulations indicate, as we will see, this is the case.

If the incident light impinges the sample along a high symmetric axis of the PC, the in-plane symmetry of the bulk eigenmodes can be used to reduce the overcounting. However, along the high symmetric axis, the superprism effect does not take place, because the group velocity vector is parallel to the axis irrespective of frequency. Thus, only the boundary condition of the field strength serves for this purpose. As a consequence a natural question arises: how can we impose the boundary condition on the bulk eigenstates? In principle, we can solve this problem by considering the resonant band structure[14,15] of the semi-infinite sample and by relating it to the band structure in bulk. Instead, below we propose an alternative method to explore the coupling.

The layer-KKR method[16–19] can serve for this purpose. In this method both the transmission spectrum through a finite slab and the band structure of PC's composed of a regular array of nonoverlapping spheres in a host can be calculated very accurately in an unified manner by using the scattering matrices of a monolayer of spheres as input ingredient. If the slab thickness is large enough, the electromagnetic field in the deepest region of the slab can be regarded as a superposition of the true bulk eigenstates α; in other words, the field at the region is not affected by the finite size of the sample. Thus, instead of imposing the boundary condition, the calculation of the superposition coefficients c_α gives an estimation of the coupling. In addition, the coefficients have a direct physical meaning, that is, they give the branching ratio (BR) of the bulk eigenstates

$$\mathrm{BR}_\alpha=\frac{|c_\alpha|^2}{\sum_{\alpha'}|c_{\alpha'}|^2}, \tag{7}$$

where the summation is over all the bulk eigenmodes satisfying the kinetic matching conditions. The coefficients can be evaluated by a kind of overlapping integral between the field excited in the bulk by the incident light and the actual eigenstates of the infinite PC as explained below.

In the layer-KKR method the photonic band structure is obtained by

$$\begin{pmatrix} Q_{++}-Q_{+-}Q_{--}^{-1}Q_{-+} & Q_{+-}Q_{--}^{-1} \\ -Q_{--}^{-1}Q_{-+} & Q_{--}^{-1}\end{pmatrix}\begin{pmatrix}u^+(N)\\ u^-(N)\end{pmatrix} = e^{ik_zd}\begin{pmatrix}u^+(N)\\ u^-(N)\end{pmatrix}, \tag{8}$$

where $u^\pm(N)$ is the column vector composed of the Fourier coefficients of the forward $(+)$ and backward $(-)$ propagating modes in the electric field in the space (void) between the $(N-1)$-th and Nth layers as

$$u^\pm(N)=\begin{pmatrix}\mathbf{u}^\pm_{\mathbf{h}_1}(N)\\ \mathbf{u}^\pm_{\mathbf{h}_2}(N)\\ \vdots\end{pmatrix}, \tag{9}$$

$$\mathbf{E}_{\rm void}(\mathbf{r})=\sum_{\mathbf{h}}\mathbf{u}^+_{\mathbf{h}}(N)e^{i\mathbf{K}^+_{\mathbf{h}}\cdot\mathbf{r}}+\mathbf{u}^-_{\mathbf{h}}(N)e^{i\mathbf{K}^-_{\mathbf{h}}\cdot\mathbf{r}}, \tag{10}$$

$$\mathbf{K}^\pm_{\mathbf{h}}=\mathbf{k}_\parallel+\mathbf{h}\pm\hat{z}\sqrt{\epsilon_{\rm void}\frac{\omega^2}{c^2}-(\mathbf{k}_\parallel+\mathbf{h})^2}. \tag{11}$$

Here, $\mathbf{h}$ denotes the 2D reciprocal lattice vector associated to the 2D periodicity on the surface, $k_\parallel\equiv(k_x,k_y)$ is the wave vector within the SBZ, and $\epsilon_{\rm void}$ is the dielectric constant of the void. In Eq. (8) Q's are the scattering matrices of the monolayer[17] which relate $u^\pm(N)$ with $u^\pm(N+1)$ as

$$\begin{pmatrix}u^+(N+1)\\ u^-(N)\end{pmatrix}=\begin{pmatrix}Q_{++} & Q_{+-}\\ Q_{-+} & Q_{--}\end{pmatrix}\begin{pmatrix}u^+(N)\\ u^-(N+1)\end{pmatrix}. \tag{12}$$

Let us denote Eq. (8) simply as $Tu(N)=e^{ik_zd}u(N)$. In this equation T is equal to the transfer matrix which relates $u(N)$ with $u(N+1)$ as

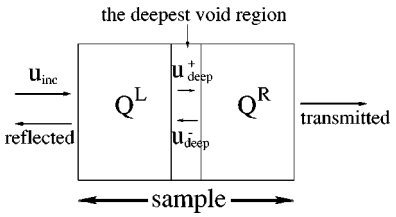

FIG. 2. Schematic illustration of the geometry used in the calculation of the branching ratio.

$$u(N+1)=Tu(N). \tag{13}$$

Since T is not Hermitian, the left eigenstate u_L of T is generally different from the complex conjugate of the right eigenstate u_R. Assume that these are normalized as

$$(u_L^{\alpha})^{\dagger}u_R^{\alpha'}=\delta_{\alpha\alpha'}. \tag{14}$$

The coupling of the actual eigenstate with real $k_z^{(\alpha)}$, is estimated by the overlapping

$$c_{\alpha}=(u_L^{\alpha})^{\dagger}u_{\mathrm{deep}}, \tag{15}$$

where u_{deep} is a column vector which contains the Fourier coefficients of the electric field excited by the incident light in the deepest void region of the sample and is defined by

$$u_{\mathrm{deep}}=\begin{pmatrix} u^{+}_{\mathrm{deep}} \\ u^{-}_{\mathrm{deep}} \end{pmatrix}=\begin{pmatrix} 1 \\ Q^R_{-+} \end{pmatrix}(1-Q^L_{+-}Q^R_{-+})^{-1}Q^L_{++}u_{\mathrm{inc}}. \tag{16}$$

In the above equation u_{inc} is the column vector which corresponds to the incident light as

$$u_{\mathrm{inc}}=\begin{pmatrix} \mathbf{u}_{\mathrm{inc},\mathbf{h}_1} \\ \mathbf{u}_{\mathrm{inc},\mathbf{h}_2} \\ \vdots \end{pmatrix}, \tag{17}$$

$$\mathbf{E}_{\mathrm{inc}}(\mathbf{r})=\sum_{\mathbf{h}} \mathbf{u}_{\mathrm{inc},\mathbf{h}}e^{i\mathbf{K}^{+}_{h}\cdot\mathbf{r}}, \tag{18}$$

and Q^L, Q^R are the scattering matrices for the front-half and rear-half layers of the sample as is depicted in Fig. 2.

In Eq. (15) there is a selection rule on the spatial symmetry of the electric field. Since the transfer matrix T commutes with the symmetry operations of the point group relevant to the incident k vector, the eigenstates of T are classified according to the irreducible representations of the point group. Thus, c_{α} becomes zero if u_{bulk} is attributed to the different irreducible representation from that of u_L^{α}. As an example, in what follows we estimated the BR of the bulk eigenstates when the incident $\mathbf{k}$ vector lies in a mirror plane.

Let us consider incident light whose $\mathbf{k}_{\parallel}$ component coincides with the M point of the SBZ. Following the procedure explained above we employed a 32-monolayers slab of the bare opal along the (111) direction to calculate the electric field in the space between the 16th and 17th layer, where the bulk configuration is assumed to be achieved. At the same time, the photonic dispersion relation of the fully periodic system is also calculated along k_z with the same $\mathbf{k}_{\parallel}$ wave vector. In Fig. 3 we show such dispersion relation in the high frequency region [0.9–1.2] where many bands appear due to folding effects. Now, let us discuss the case of one frequency in a multibranching regime; for example, $\omega a/(2\pi c)=1.0$. At this frequency Fig. 3 shows that there are four eigenstates which are kineticly matched to the incident light; i.e., the ones with positive slope. However, if the incident light is S polarized, that is, the polarization vector of the electric field is parallel to the boundary, its symmetry under the mirror reflection is odd. On the other hand, the bulk eigenstates are also classified by the parity of the mirror reflection. Thus, bulk eigenmodes with even parity can not couple to the incident light. This fact is confirmed by calculating the magnitude of $|c_{\alpha}|^2$. The values $|c_{\alpha}|^2$ of the even eigenmodes (thin lines in Fig. 3) are less than 10^{-15}, whereas those of the odd eigenmodes (thick lines in Fig. 3) are 0.0017 and 0.9665. At this point we have to notice that modes with negative slope also contributes to the field u_{bulk} in Eq. (13) because of the finite size of the sample; their $|c_{\alpha}|^2$ values are 0.0011 and 0.048 at this frequency. Nevertheless, the values of the negative component will not been taking into account to calculate the BR associated to the semi-infinite system we are considering here. Thus, the BR of the dominant mode at the working frequency is about 99.8%. This kind of dominance in the BR is found in a large region of $(\omega,\mathbf{k}_{\parallel})$ and it is very useful for technological applications. Figure 3 also includes the BR values at the frequency 1.15 (in red. units) where mainly two bands are excited by the incident light, being their BR's 32 and 67 %. The remaining 1% is associated to the rest of the bands satisfying the kinetic matching conditions.

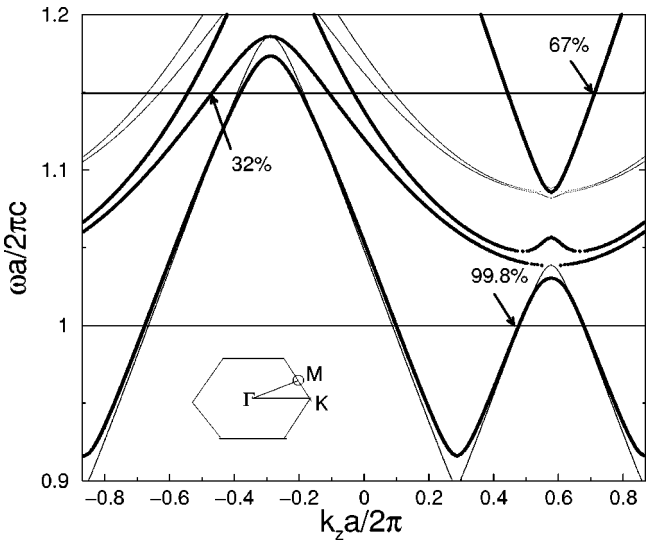

FIG. 3. The photonic band structure of the bare opal at the M point in the SBZ of the fcc (111) surface. Eigenmodes have even parity (thin lines) or odd parity (thick lines) with respect to the mirror plane which contains M. The branching ratio of the eigenmodes at $\omega a/2\pi c=1.0,1.15$ (horizontal lines) are given.

We must remark the the procedure described above is applicable with slight modifications in the the Pendry's transfer matrix method.[20] The group velocity of the bulk eigenmodes can be calculated in this method by taking the spatial

average of the Poynting vector of the eigenmode in a unit cell. However, since the method is based on finite differentiation of Maxwell's equation, the results at high frequencies are dubious compared to the layer-KKR method.

IV. RESULTS AND DISCUSSION

The method described in the previous sections were examined numerically for the bare opal system. In order to obtain the group velocity, which is very difficult in the layer-KKR method, a combined use of the plane wave expansion method and the layer-KKR is needed. In the plane wave expansion method the group velocity can be easily calculated by the Hellman-Feynmann theorem.

At a given polar and azimuthal angles as well as frequency of the incident light, we first calculated the band structure and the coupling c_α of the bulk eigenstates by the layer-KKR method (see Sec. III). Since the layer-KKR method is a kind of ''on-shell'' method, k_z, which is the normal component of the Bloch wave vector to the boundary surface, is obtained as the output. Among the actual bulk eigenstates with real k_z^α we select the ones with the largest $|c_\alpha|^2$. By using the wave vector $(\mathbf{k}_\parallel, k_z)$ of the leading one as the input, the band structure along with the group velocity was calculated by the *E* method of the plane wave expansion. After confirming that (a) there is the eigenmode whose frequency is near to the input frequency within 1% of error and that (b) v_z of the eigenmode is positive, we calculated the polar and azimuthal angle of the propagating light inside the photonic crystal by Eq. (6). In case that condition (b) is not satisfied, we selected the next leading $k_z^{(\alpha)}$ as the input in the plane wave expansion and recalculated the eigenfrequency and the group velocity.

In the plane wave expansion 537 reciprocal lattice vectors were used. The convergence is good even with this rather small number of reciprocal lattice vectors because of the small index contrast between the spheres and air. As for the layer-KKR method we used spherical harmonics up to $l_{\max}=6$ and 37 reciprocal lattice vectors relevant to SBZ. A good convergence is also obtained with these values.

First, let us consider the superprism effect near the edge of a pseudogap. It is well known that a pseudogap opens between the second and third bands along the Γ-L direction in the fcc Brillouin zone; i.e., at the Γ point of the SBZ associated with the surface normal to (111) [see inset of Fig. 1(a)]. The gap still opens if the reduced wave vector on SBZ is apart from the Γ point, as was shown in Fig. 1. In Fig. 4 θ_{out} is plotted as a function of frequency. Here, the boundary surface is normal to the (111) direction and the polar and azimuthal angles of the *S*-polarized incident light are $\theta_{\text{inc}}=10°$ and $\phi_{\text{inc}}=-20°$, respectively. In this parametrization of θ_{inc} and ϕ_{inc}, the positive x axis is parallel to the $(\bar{1}10)$ direction and accordingly the positive y axis is parallel to $(\bar{1}\bar{1}2)$.

At the edge of the pseudogap v_z becomes zero, so that θ_{out} generally reaches up to 90° irrespective of v_x, v_y. This behavior is clearly seen in Fig. 4 below the band gap [i.e., at $\omega a/(2\pi c)\simeq 0.65$] and above it. Figure 4 also shows that

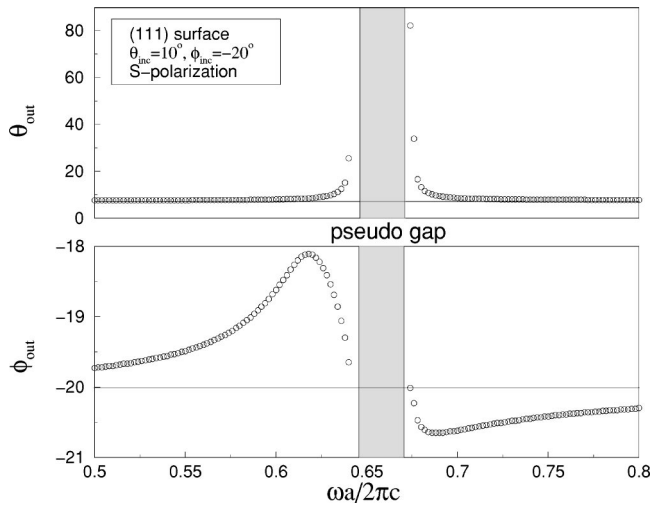

FIG. 4. The superprism effect in a bare opal sample cut along the (111) surface at low frequencies. The incident direction is fixed at $(\theta_{\text{inc}}, \phi_{\text{inc}})=(10°, -20°)$. The horizontal lines represents the results obtained by the Snell's law using a spatially averaged dielectric constant. Notice how the polar angle inside the photonic crystal shows a large sensitivity to frequency near the pseudogap edges.

Snell's law with the spatially averaged dielectric constant

$$\sin\theta_{\text{out}}=\frac{1}{n_{\text{av}}}\sin\theta_{\text{inc}}, \tag{19}$$

works fairly well in the remaining part of the displayed frequency region. In bare opals $n_{\text{av}}\simeq 1.35$ and thus at $\theta_{\text{inc}}=10°$ one obtains $\theta_{\text{out}}=7.33°$, which is represented by the thin horizontal line in Fig. 4, As for ϕ_{out}, it is observed that the deviation from Snell's law ($\phi_{\text{out}}=\phi_{\text{inc}}$) is small. Therefore, the superprism effect obtained near the pseudogap could be used as a frequency-selector device.

Next, let us discuss the superprism effect in the frequency region where several eigenmodes are kineticly matched to the incident light. Now, the BR of bulk eigenmodes varies with the frequency. In most of the cases examined the ratio of the leading modes is greater than 30% and there are many modes whose BRs are less than a few percent. Similar results in experiments were reported.[3] In this region the superprism effect appears quite generally at any angle of incidence. This is due to the huge anisotropy of the flat bands which exist in this region due to folding effects. In Fig. 5 the propagating direction inside the opal $(\theta_{\text{out}}, \phi_{\text{out}})$ is plotted as a function of frequency for a given incident direction. Here, the boundary surface and the coordinate system is the same as in Fig. 4. The polar and azimuthal angles, which define the incident light are $\theta_{\text{inc}}=40°$ and $\phi_{\text{inc}}=-20°$, respectively. In contrast to the superprism effect near the pseudogap (see Fig. 4), now ϕ_{out} also reveals large sensitivity to frequency; in fact $\Delta\phi_{\text{out}}\simeq 100°$ for $\Delta\omega\simeq 0.1$ (in red. units). Also, it can be observed a split of the incident beam inside the opal for frequencies above $\omega a/(2\pi c)=1.1$. This phenomenon is caused by the fact that two eigenmodes are coupled to the incident light with a similar strength. The resulting bifurca-

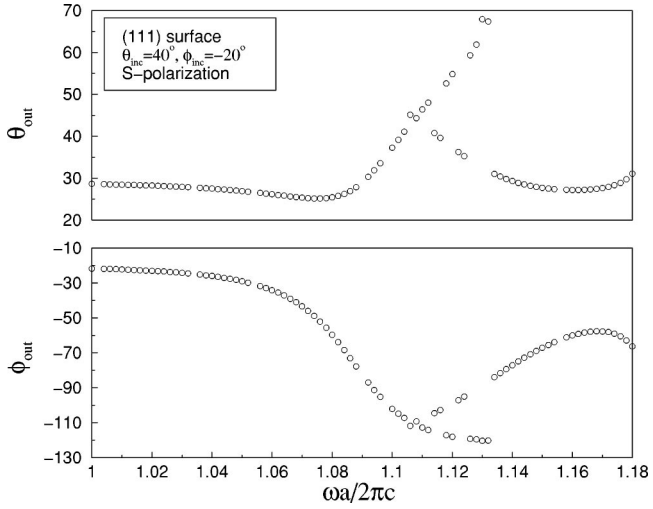

FIG. 5. The superprism effect for a bare opal sample cut along the (111) surface at high frequencies. The incident direction is fixed at $(\theta_{\rm inc},\phi_{\rm inc})=(40°,-20°)$. Both the polar and azimuthal angles defining the propagating direction inside the opal show a large sensitivity to frequency.

tion of the light serves as the beam splitter in which the intensities of the two beams are almost the same.

To conclude, Fig. 6 shows the results for the superprism effect when the boundary surface is normal to the (001) direction. As it is known, the pseudogap between the second and the third bands, which are doubly degenerate in Δ [i.e., the Γ point in the SBZ of the fcc (001) surface][see Fig. 1(b)] is very small in comparison to the (111) case [see Fig. 1(a)]. Therefore, a fine tuning of frequency is necessary in order to get the superprism effect near the first (001) pseudogap. Nevertheless, the superprism effect also appears quite generally in the frequency region where many flat bands exist.

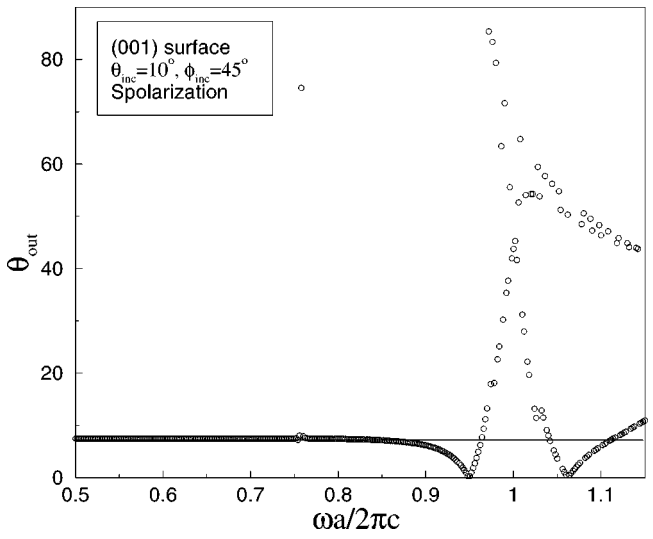

FIG. 6. The superprism effect for a bare opal cut along the fcc (001) surface. The incident direction is fixed at $(\theta_{\rm inc},\phi_{\rm inc})=(10°,45°)$. The horizontal line represents the Snell's law with a average dielectric function.

The incident direction is fixed at every frequency by the following polar and azimuthal angles $\theta_{\rm inc}=10°$ and $\phi_{\rm inc}=45°$, respectively. Here, the azimuthal angle is defined with respect to a (x,y) set of axis in which the positive x axis is parallel to $(\bar{1}10)$ and the positive y axis is parallel to (110). In addition, the numerical simulation shown in Fig. 6 corresponds to the case in which the $\mathbf{k}_{\parallel}$ lies in a mirror plane of the group C_{4v}, which is the relevant symmetry group in the fcc (001) plane. As a consequence, $\phi_{\rm out}$ must be 45° or $-135°$, values that were confirmed by our numerical simulation. The output polar angle reveals a remarkable sensitivity to frequency. In a similar manner than in the (111) case (see Fig. 4) $\theta_{\rm out}$ shows a huge frequency dependence in a narrow region close to the edges of the pseudogap. In contrast, the superprism effect around $\omega a/(2\pi c)=1$ and above is more pronounced than in the (111) case; now three branches with an almost same order of coupling strength. This effect indicates that inside the photonic crystal the incident beam splits into three beams with almost equal intensity will be observed. It is interesting to remark that among the three branches the lowest one propagates exactly along the very same (001) direction when $\omega a/2\pi c\simeq 1.05,0.95$.

V. SUMMARY

In this paper the superprism effect is theoretically investigated in bare opals with the boundary surface normal to the (111) or (001) direction. The bare opals, which consist of a closed-packed fcc structure of silica spheres in air are the simplest opal-based 3D photonic crystals. The direction of light propagation inside the opal is determined by the group velocity of the eigenmodes which are kineticly matched with the incident light and have the largest coupling with the field excited by the incident light. We have observed two remarkable frequency regions in which the superprism effect takes place. One is near the edges of pseudogaps and the other is the region where many flat bands exist. In the latter region the effect takes place quite generally due to the enhanced anisotropy of the bands. Our numerical simulations demonstrated that many eigenmodes can be weekly coupled to the incident light. We have particularly emphasized the symmetry characters of the opal crystals, because they impose a strong limitation of the direction of propagation and are applicable to other kinds of photonic crystals consisting of fcc arrays of spheres. This work predicts many interesting application of bare opal systems such as frequency selector devices as well as beam splitters. It is hoped that these predictions stimulates further experiments having these goals.

ACKNOWLEDGMENTS

The authors would like to thank C. López for valuable discussions and N. Stefanou for providing their layer-KKR code. This work was supported by European Community under Project No. PHOBOS IST-1999-19009 and by the Spanish CICyT Project No. MAT2000-1670-C04-04. We also acknowledge the computing facilities provided by the Centro de Computación Científica at Universidad Autónoma de Madrid.

[1] E. Yablonovitch, Phys. Rev. Lett. **58**, 2059 (1987).
[2] H. Kosaka, T. Kawashima, A. Tomita, M. Notomi, T. Tamamura, T. Sato, and S. Kawakami, Phys. Rev. B **58**, R10 096 (1998).
[3] M. Notomi, Phys. Rev. B **62**, 10 696 (2000).
[4] M. Notomi, T. Tamamura, Y. Ohtera, O. Hanaizumi, and S. Kawakami, Phys. Rev. B **61**, 7165 (2000).
[5] L. Zavieh and T.S. Mayers, Appl. Phys. Lett. **75**, 2533 (1999).
[6] R.D. Pradhan, J.A. Bloodgood, and G.H. Watson, Phys. Rev. B **55**, 9503 (1997).
[7] F. Meseguer, H. Miguez, A. Blanco, and C. Lopez, Recent Results Dev. App. Phys. **2**, 327 (1999) and references therein.
[8] H. Miguez, F. Meseguer, C. López, F. López-Tejeira, and J. Sánchez-Dehesa, Adv. Mater. **13**, 393 (2001).
[9] A. Blanco, E. Chomski, S. Grabtchak, M. Ibisate, S. John, S.W. Leonard, C. López, F. Meseguer, H. Miguez, J.P. Mondia, G.A. Ozin, O. Toader, and H.M. van Driel, Nature (London) **405**, 437 (2000).
[10] H. Míguez, F. Meseguer, C. López, M. Holgado, G. Andreasen, A. Mifsud, and F. Fornés, Langmuir **16**, 4405 (2000).
[11] A. Blanco, C. López, F. Meseguer, F. López-Tejeira, and J. Sánchez-Dehesa, Appl. Phys. Lett. **78**, 3181 (2001).
[12] H.S. Sozuer, J.W. Haus, and R. Inguva, Phys. Rev. B **45**, 13 962 (1992).
[13] K. Busch and S. John, Phys. Rev. E **58**, 3896 (1998).
[14] H. Miyazaki and K. Ohtaka, Phys. Rev. B **58**, 6920 (1998).
[15] K. Ohtaka, Y. Suda, S. Nagano, T. Ueta, A. Imada, T. Koda, J.S. Bae, K. Mizuno, S. Yano, and Y. Segawa Phys. Rev. B **61**, 5267 (2000).
[16] N. Stefanou, V. Karathanos, and A. Modinos, J. Phys.: Condens. Matter **4**, 7389 (1992).
[17] N. Stefanou, V. Yannopapas, and A. Modinos, Comput. Phys. Commun. **113**, 49 (1998); **132**, 189 (2000).
[18] K. Ohtaka, and Y. Tanabe, J. Phys. Soc. Jpn. **65**, 2276 (1996).
[19] K. Ohtaka, T. Ueta, and K. Amemiya, Phys. Rev. B **57**, 2550 (1998).
[20] J.B. Pendry and A. MacKinnon, Phys. Rev. Lett. **69**, 2772 (1992).